The Function of RH22, a DEAD RNA Helicase, in the Biogenesis of the 50S Ribosomal Subunits of Arabidopsis Chloroplasts[1][W][OA]

Wei Chi, Baoye He, Juan Mao, Qiannan Li, Jinfang Ma, Daili Ji, Meijuan Zou, and Lixin Zhang*

Photosynthesis Research Center, Key Laboratory of Photobiology, Institute of Botany, Chinese Academy of Sciences, Beijing 100093, China

The chloroplast ribosome is a large and dynamic ribonucleoprotein machine that is composed of the 30S and 50S subunits. Although the components of the chloroplast ribosome have been identified in the last decade, the molecular mechanisms driving chloroplast ribosome biogenesis remain largely elusive. Here, we show that RNA helicase 22 (RH22), a putative DEAD RNA helicase, is involved in chloroplast ribosome assembly in Arabidopsis (*Arabidopsis thaliana*). A loss of *RH22* was lethal, whereas a knockdown of *RH22* expression resulted in *virescent* seedlings with clear defects in chloroplast ribosomal RNA (rRNA) accumulation. The precursors of 23S and 4.5S, but not 16S, rRNA accumulated in *rh22* mutants. Further analysis showed that RH22 was associated with the precursors of 50S ribosomal subunits. These results suggest that RH22 may function in the assembly of 50S ribosomal subunits in chloroplasts. In addition, RH22 interacted with the 50S ribosomal protein RPL24 through yeast two-hybrid and pull-down assays, and it was also bound to a small 23S rRNA fragment encompassing RPL24-binding sites. This action of RH22 may be similar to, but distinct from, that of SrmB, a DEAD RNA helicase that is involved in the ribosomal assembly in *Escherichia coli*, which suggests that DEAD RNA helicases and rRNA structures may have coevolved with respect to ribosomal assembly and function.

Given the prokaryotic origin of chloroplasts, the protein-synthesizing systems of chloroplasts are often considered to be very similar to those of bacteria. Chloroplasts contain 70S ribosomes, which are similar to prokaryotic ribosomes and distinct from their cytosolic counterparts, 80S ribosomes. The ribosomal RNAs (rRNAs) of higher plant chloroplasts are highly conserved and are most closely related to bacterial sequences (Branlant et al., 1981; Harris et al., 1994). The 30S subunit comprises 16S rRNA in chloroplasts and *Escherichia coli*. However, the 50S subunit of chloroplast ribosomes is composed of three rRNAs (23S, 4.5S, and 5S rRNAs), rather than the 23S and 5S rRNAs of *E. coli* (Harris et al., 1994). In chloroplasts, the 16S, 23S, 4.5S, and 5S rRNAs are encoded in an operon and are synthesized as a single large precursor (Edwards and Kössel, 1981). Maturation of the primary transcript occurs via multiple steps, including nucleotide modifications as well as endonucleolytic and exonucleolytic cleavages that sequentially remove the precursor sequences (Strittmatter and Kössel, 1984; Walter et al., 2002; Bollenbach et al., 2005).

Although the overall structural organization of the ribosome has been described in great detail (Ban et al., 2000; Schluenzen et al., 2000; Yusupov et al., 2001), the molecular mechanisms involved in ribosomal biogenesis have not yet been resolved. In *E. coli*, the biogenesis of ribosomal subunits is a stepwise process that comprises the processing and folding of the pre-rRNA and its concomitant assembly with the ribosomal proteins (Gourse et al., 1996; Cheng and Deutscher, 2003; Holmes and Culver, 2005). Precursor particles that consist of a subset of ribosomal proteins, as well as rRNA precursors, are formed during this process (Lindahl, 1975). The isolation and characterization of these precursor particles enabled mapping of the basic series of events of ribosome assembly in *E. coli* (Nierhaus, 1991; Williamson, 2003). In chloroplasts, however, the existence of such precursor particles has not been fully proven (Dorne et al., 1984). Thus, our knowledge of many important aspects of chloroplast ribosome biogenesis is still limited, especially regarding the coordination of the processing and modification of the rRNA to ensure its correct structural assembly with ribosomal proteins.

Ribosomal biogenesis depends on a large number of nonribosomal factors that confer directionality and accuracy in this process (Fromont-Racine et al., 2003; Henras, et al., 2008; Shajani et al., 2011). Genetic approaches have been used to identify mutants that

[1] This work was supported by the National Natural Science Foundation of China (grant no. 31070213), the Major State Basic Research Development Program (grant no. 2009CB118500), and the Transgenic Research Program of the Ministry of Agriculture of China (grant no. 2011ZX08009–003–005)

* Corresponding author; e-mail zhanglixin@ibcas.ac.cn.

The author responsible for distribution of materials integral to the findings presented in this article in accordance with the policy described in the Instructions for Authors (www.plantphysiol.org) is: Lixin Zhang (zhanglixin@ibcas.ac.cn).

[W] The online version of this article contains Web-only data.

[OA] Open Access articles can be viewed online without a subscription.

www.plantphysiol.org/cgi/doi/10.1104/pp.111.186775

are defective in ribosome biogenesis in *E. coli*, and these studies have uncovered a considerable number of nonribosomal factors that are involved in the process, including AAA-ATPases, GTPases, kinases, chaperone proteins, and RNA helicases (Kaczanowska and Rydén-Aulin, 2007; Shajani et al., 2011). These factors play important roles in the transcription and processing of preribosomal RNAs as well as in their proper folding and assembly with ribosomal proteins (Kaczanowska and Rydén-Aulin, 2007). In higher plants, several mutants that are defective in chloroplast ribosome biogenesis have been isolated, and most of these are defective in rRNA processing (Barkan, 1993; Walter et al., 2002; Bellaoui et al., 2003; Bisanz et al., 2003; Kishine et al., 2004; Bollenbach et al., 2005; Schmitz-Linneweber et al., 2006; Koussevitzky et al., 2007; Watkins et al., 2007; Beick et al., 2008; Beligni and Mayfield, 2008; Yu et al., 2008; Zybailov et al., 2009; Nishimura et al., 2010). However, the molecular mechanisms responsible for regulating rRNA processing and ribosomal biogenesis in most of the identified mutants are not fully understood.

DEAD-box family RNA helicases are characterized by the presence of at least nine conserved motifs and are named for the highly conserved Asp-Glu-Ala-Asp residues in motif II (Caruthers and McKay, 2002; Cordin et al., 2006). These proteins are generally believed to unwind or rearrange local RNA secondary structures using energy released from ATP hydrolysis (Caruthers and McKay, 2002; Cordin et al., 2006). However, it was recently shown that in several cases, these enzymes may assist in the correct folding of RNA by acting as RNA "chaperones" or promoting the dissociation of RNA and protein molecules (Jankowsky and Fairman, 2007). The DEAD RNA helicases participate in nearly every process that involves RNA synthesis, RNA modification, RNA cleavage, RNA degradation, ribosome biogenesis, and translation initiation (Silverman et al., 2003; Cordin et al., 2006). They are widely distributed in organisms, and many DEAD RNA helicase proteins are associated with ribosome biogenesis in eukaryotes and prokaryotes (de la Cruz et al., 1999; Kressler et al., 1999; Iost and Dreyfus, 2006). Five DEAD RNA helicase proteins have been identified in *E. coli* (RhlB, CsdA, DpbA, RhlE, and SrmB). SrmB and CsdA, and probably DbpA, are required for the formation of functional ribosome subunits (Kossen and Uhlenbeck, 1999; Charollais et al., 2003, 2004). It has been proposed that both SrmB and CsdA are involved in the assembly of the 50S rather than the 30S ribosomal subunit (Charollais et al., 2003, 2004).

DEAD RNA helicases have also been identified in the chloroplast of higher plants. The tobacco (*Nicotiana tabacum*) chloroplast DEAD RNA helicase VDL is involved in the early differentiation of chloroplasts, but its precise function remains unclear (Wang et al., 2000). There are 32 DEAD RNA helicases in Arabidopsis (*Arabidopsis thaliana*), which are named AtRH1 to AtRH32 (Aubourg et al., 1999). More than 10 of these proteins have been predicted to be localized to chloroplasts by TargetP prediction analysis, and RH39, RH3, RH22, RH26, and RH50 have been detected in chloroplast fractions in proteomic analyses (Zybailov et al., 2008). Herein, we demonstrate that one of these chloroplast DEAD RNA helicases, RH22, plays an important role in the biogenesis of the chloroplast ribosome.

RESULTS

RH22 Is a Chloroplast DEAD Box Protein

RH22 is a putative DEAD-box RNA helicase with a 58-amino acid transit peptide that is predicted to be targeted to the chloroplast, according to the TargetP program. To confirm the chloroplast localization of RH22, a chimeric construct consisting of the coding region of RH22 fused to GFP and expressed under the control of the 35S cauliflower mosaic virus promoter was generated and transiently expressed in the protoplasts of Arabidopsis mesophyll cells. We observed GFP signals by confocal laser-scanning microscopy and found that the fusion protein colocalized with chloroplastic chlorophyll in the mesophyll cells, consistent with the results obtained for GFP fused to the transit peptide of the small subunit of Arabidopsis ribulose bisphosphate carboxylase (Fig. 1A). The fluorescence signals were dispersed in the cytosol and the nucleus when protoplasts were transformed with a control vector without a specific targeting sequence (Fig. 1A). Thus, these findings indicate that RH22 localizes to the chloroplast.

RH22 is widely expressed in most Arabidopsis tissues, including leaves, stems, roots, siliques, and flowers, as revealed by RNA-blot analysis (Fig. 1B). However, *RH22* transcript accumulation was relatively higher in leaves than in other tissues. The expression of *RH22* appeared to be closely associated with the age and developmental stages of the Arabidopsis leaves, occurring primarily during early stages of development. The *RH22* transcripts accumulated at the highest levels in 4-d-old seedlings and were significantly reduced in 8-d-old seedlings (to approximately 20% of the level detected in 4-d-old seedlings; Fig. 1C). Nevertheless, the levels of *RH22* transcript in 12-d-old seedlings were only slightly reduced compared with those in 8-d-old seedlings (Fig. 1C). To examine the effects of light on the expression of *RH22* in Arabidopsis, the levels of *RH22* transcripts in the leaves of dark-adapted plants were compared with those in plants illuminated with white light after dark adaptation. As shown in Figure 1D, *RH22* transcripts accumulated at very low levels in dark-adapted plants and increased upon illumination, similar to the pattern in plants under continuous light.

Knockdown of *RH22* Leads to a Delayed-Greening Phenotype in Arabidopsis

We obtained three T-DNA insertion alleles of *RH22* from the Arabidopsis Biological Resource Center (ABRC) and named them *rh22-1* (Salk_032399), *rh22-2* (Salk_065388C), and *rh22-3* (CS856759). The T-DNA

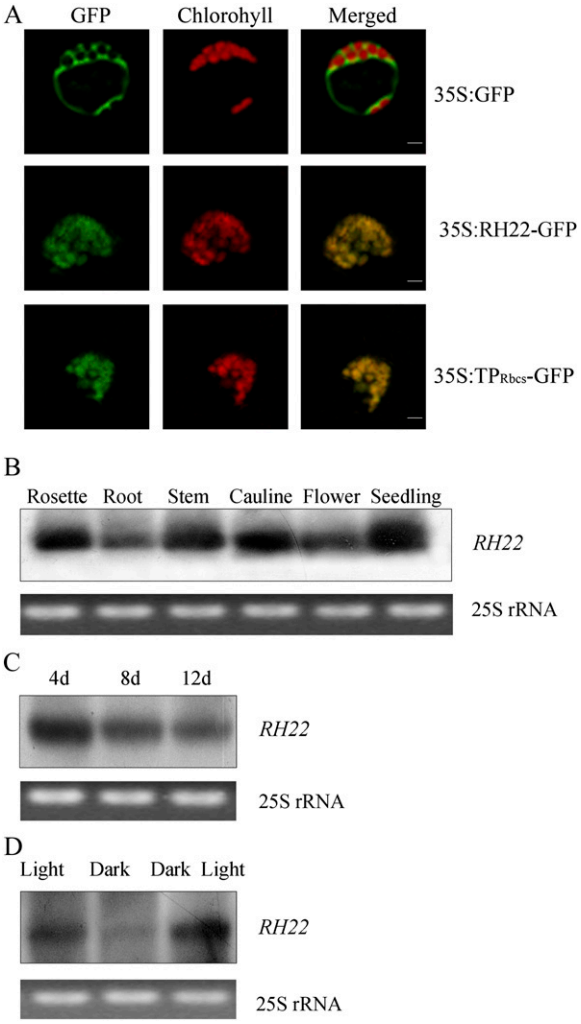

Figure 1. Subcellular localization and expression patterns of RH22. A, Chloroplast localization of RH22, as demonstrated by GFP assays. The fluorescence signals were visualized using confocal laser-scanning microscopy. Green indicates GFP fluorescence, red shows chloroplast autofluorescence, and orange/yellow indicates regions where the two types of fluorescence merged. Top row, GFP signals from a control lacking the transit peptide; middle row, the RH22-GFP fusion protein; bottom row, the transit peptide of the ribulose bisphosphate carboxylase small subunit (control). Bars = 5 μm. B, *RH22* transcript levels in different organs of Arabidopsis determined by RNA gel-blot analysis. Approximately 10 μg of RNA from rosettes, roots, stems, caulines, flowers, and seedlings of 4-week-old wild-type plants were subjected to RNA gel blotting. The 25S rRNA stained with ethidium bromide is shown as a loading control. C, Transcript levels of *RH22* in Arabidopsis leaves at 4, 8, and 12 d. D, Light-induced accumulation of *RH22* transcripts. Three-week-old plants were grown under light, dark-adapted for 24 h, or illuminated for 3 h after a 24-h dark adaptation.

insertions in *rh22-1* and *rh22-2* were in introns 6 and 7, respectively, and *rh22-3* was in exon 1 (Fig. 2A). The homozygous *rh22-1* and *rh22-2* mutant plants exhibited a high-chlorophyll-fluorescence phenotype in a developmentally regulated manner, similar to that of *dg1* (Chi et al., 2008). As shown in Figure 2B, the growth of *rh22-1* was retarded, and 10-d-old cotyledons displayed an obvious pale-green phenotype under normal growth conditions. The analysis of the chlorophyll fluorescence kinetics showed that the ratio of the variable fluorescence to the maximum fluorescence (F_v/F_m), which reflects the maximum potential of PSII photochemical reactions, was significantly lower in the *rh22-1* cotyledons than in wild-type plants (Fig. 2B). After growth for 20 d, the cotyledons of *rh22-1* gradually turned green, and the F_v/F_m ratios gradually increased and approached the wild-type levels (0.8), but the newly emerging true leaves showed the pale-green phenotype (Fig. 2B). The *rh22-2* mutant had a phenotype similar to that of *rh22-1*, but its chlorosis and growth retardation were less severe. After growth for 10 d, only the newly emerging true leaves following the cotyledons of *rh22-2* were pale green; the cotyledons of *rh22-2* were restored to wild-type levels (Fig. 2B). Electron microscopic analysis of chloroplasts from wild-type and mutant plants of 10-d-old seedlings showed that the chloroplasts of wild-type cotyledons had well-structured thylakoid membranes that were composed of grana connected by stroma lamellae, whereas those of *rh22-1* cotyledons had fewer stacked thylakoids and exhibited a disturbed thylakoid membrane organization (Supplemental Fig. S1). These data suggest that the *rh22* mutation affects chloroplast development.

The T-DNA insertions did not completely suppress *RH22* gene expression in the *rh22-1* and *rh22-2* mutants, as reverse transcription (RT)-PCR analysis showed that *At1g59990* (*RH22*) remained expressed at low levels in both of them (Fig. 2C). Using quantitative (q)RT-PCR analysis, we found that RH22 RNA was reduced to approximately 16% and 45% of the wild-type levels in *rh22-1* and *rh22-2*, respectively (Fig. 2D). Immunoblot analysis using a specific antibody raised against RH22 also showed that the mutants had reduced levels of RH22 protein (Fig. 2E).

To obtain potential null alleles of *RH22*, we analyzed the *rh22-3* mutant line, in which the T-DNA was inserted into the first exon of the *At1g59990* gene. However, no homozygous *rh22-3* plants were identified among the progeny in the crossing of heterozygous *rh22-3/RH22* plants, implying that a complete disruption of the *RH22* gene is lethal. The siliques of the *rh22-3/RH22* plant contained approximately 25% aborted seeds (Supplemental Fig. S2), indicating that *rh22-3* was a single-gene mutant. Thus, the complete absence of *RH22* may result in the embryonic lethality of abnormal seeds. Consistent with this analysis, the *RH22* locus was recently designated *EMBRYO DEFECTIVE3108* (*EMB3108*) in the database of an Arabidopsis knockout collection that includes lethal alleles (http://www.seedgenes.org/SeedGeneProfile).

Chloroplast Proteins Are Reduced, but Their mRNA Transcripts Accumulate Normally, in *rh22* Mutants

To investigate whether the accumulation of chloroplast proteins was also affected in the *rh22* mutants, the

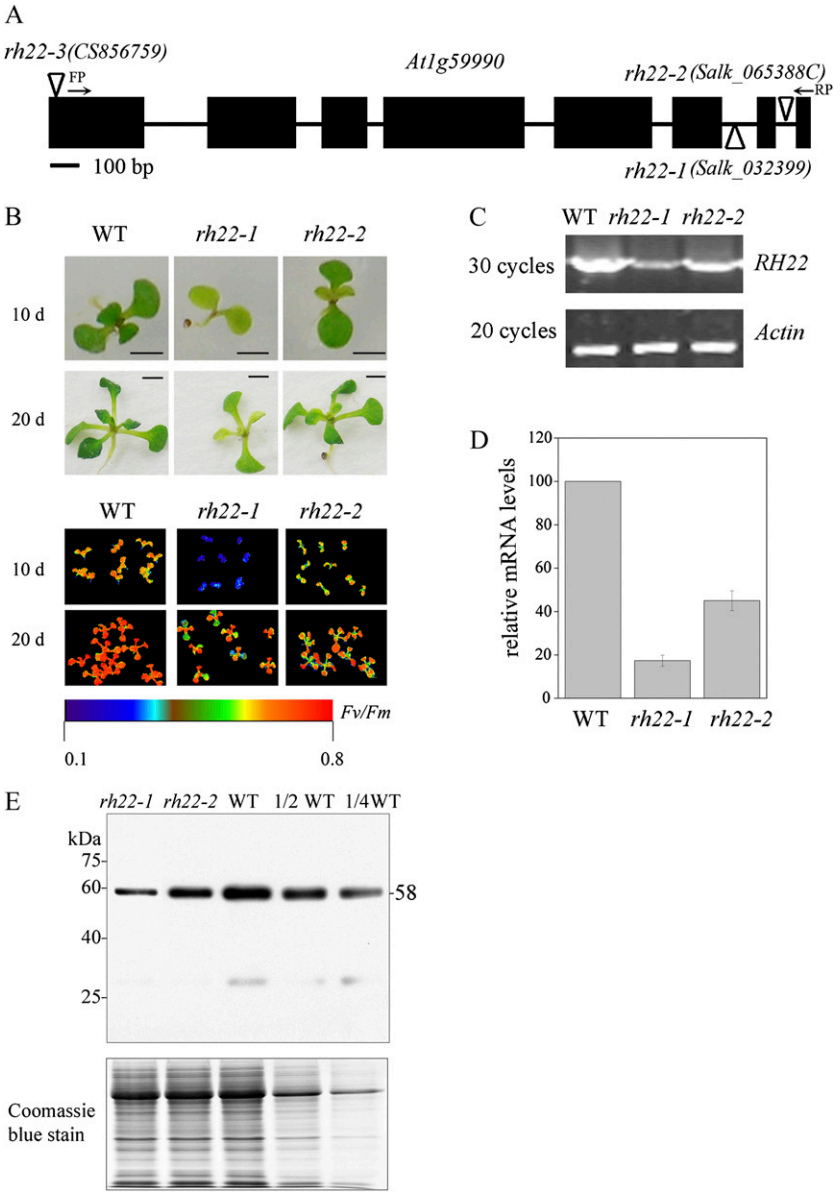

Figure 2. Phenotypes of the *rh22* mutants. A, Positions of the T-DNA insertions in the *RH22* gene. Protein-coding regions are indicated by rectangles, introns by lines, and T-DNA insertions by triangles. The arrows illustrate the primers used for the RT-PCR analysis of *RH22* mRNA shown in C. B, The phenotypes of *rh22* mutant seedlings. Photographs and chlorophyll fluorescence images show *rh22* mutants and wild-type (WT) plants grown for 10 and 20 d on Murashige and Skoog medium with 2% Suc. Fluorescence was measured with CF Imager and visualized using a pseudocolor index, as indicated at the bottom. Bars = 0.1 cm. C, Expression of *RH22* in 10-d-old *rh22-1* and *rh22-2* seedlings, as analyzed by RT-PCR. The amplification of *Actin* transcripts in the same RNA samples is shown as a control. D, Relative quantities of *RH22* in *rh22* mutants analyzed by qRT-PCR analysis. The values shown are means ± SE of three replicates. E, Immunoblot detection of RH22 in leaf extracts using the anti-RH22 antibody in wild-type and *rh22* mutant plants. Leaf extracts from 2-week-old wild-type and *rh22* seedlings (20 μg of protein, or dilutions as indicated) were separated by SDS-PAGE and probed with anti-RH22 antibodies. A replicate gel stained with Coomassie blue is shown below to provide an estimate of gel loading.

levels of representative chloroplast-encoded protein components of each of the thylakoid protein complexes in the pale-green leaves were analyzed by immunoblotting (Fig. 3). In the *rh22-1* mutant, the levels of the photosynthetic D1 and D2 reaction center proteins of PSII, the β-subunit of ATP synthase, and the cytochrome *f* protein of the cytochrome b_6f complex were reduced to approximately 25% of the wild-type levels (Fig. 3). The levels of PsaA/B, the reaction center proteins of PSI, were decreased to approximately 50% of wild-type levels (Fig. 3). The levels of these chloroplast proteins were also reduced in plants with the weaker allele, *rh22-2*, but to a lesser extent than in *rh22-1*.

The deficiencies in the levels of chloroplast-encoded proteins may be the result of defects in chloroplast transcript accumulation. To test this possibility, RNA-blot analysis of the wild-type and mutant plants was performed. No obvious differences were observed in the levels of *psbA* (encoding D1), *psbB* (encoding CP47), *psbD* (encoding D2), *atpB* (encoding CF1β), *psaA* (encoding PsaA), or *petA* (encoding cytochrome *f*) transcripts between *rh22-1* and wild-type plants (Supplemental Fig. S3).

Chloroplast rRNA Processing Is Affected in *rh22*

Although the chloroplast mRNAs examined above accumulated normally in *rh22-1*, we could not exclude the possibility that the accumulation of other chloroplast gene transcripts was affected, because these DEAD proteins are involved in RNA metabolism. To address this possibility, the abundance of global chloroplast transcripts in the *rh22-1* mutant and wild-type plants was analyzed using qRT-PCR (Supplemental

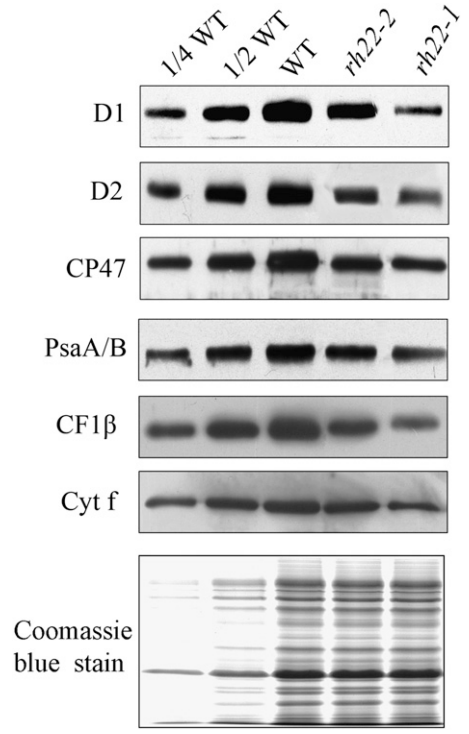

Figure 3. The accumulation of chloroplast proteins in *rh22* and wild-type (WT) plants. Immunoblot analysis of chloroplast-encoded proteins in wild-type and *rh22* mutant plants is shown. Leaf extracts were separated by SDS-PAGE and immunodetected with specific antibodies directed against D1, CP47, D2, CF1β, PsaA/B, and cytochrome *f*. A replicate gel stained with Coomassie blue is shown below to provide an estimate of gel loading.

Fig. S4). We observed no obvious differences in the levels of most of the chloroplast gene transcripts between *rh22-1* and the wild-type plants. However, the *rrn23* (23S rRNA) transcript level was increased by approximately 9-fold compared with the wild type (Supplemental Fig. S4), which indicates that the expression of *rrn23* is affected in the *rh22* mutant.

The chloroplast rRNAs are transcribed as polycistronic transcripts that undergo extensive splicing and processing to produce the mature forms. The accumulation and processing of chloroplast rRNAs was further examined by RNA gel blotting using probes specific for individual mature rRNAs (Fig. 4). When the blots were probed for 16S rRNA (probe a in Fig. 4A), mature 16S rRNA transcripts of 1.5 kb and precursor transcripts of 1.7 kb that are derived from the primary transcript by endonucleolytic cleavage in the 16S-tRNA intergenic space (Bisanz et al., 2003) accumulated in the wild-type plants (Fig. 4B). Compared with the wild-type plants, the levels of both the 1.7-kb precursors and the 1.5-kb mature transcripts were reduced in the *rh22* mutants (Fig. 4B).

In chloroplasts of Arabidopsis, the 23S-4.5S bicistronic RNA (3.2 kb) undergoes endonucleolytic cleavage to produce a mature 4.5S rRNA and a 23S precursor (2.9 kb). This 23S precursor undergoes further maturation and ultimately generates three species of 1.0, 1.2, and 0.5 kb, which represent the mature 23S transcripts after processing at hidden breaks (Bellaoui et al., 2003; Bisanz et al., 2003; Bollenbach et al., 2005). Blots probed with the 2.9-kb 23S rRNA sequence (probe b) showed that, under these conditions, the levels of the 3.2-, 2.9-, and 2.4-kb precursors were increased, but the levels of the 1.7-, 1.2-, 1.0-, and 0.5-kb bands were greatly reduced in the *rh22* mutant compared with the wild type (Fig. 4B). To confirm the altered patterns of 23S rRNA, RNA gel blots with a 2.0-kb probe targeting the 5′ end (probe c) and a 0.9-kb probe targeting the 3′ end (probe d) of the fragment were also analyzed. The mutants showed drastically increased levels of 3.2-, 2.9-, and 2.4-kb precursors. The detected PCR product spanned the hidden break at the 3′ end of the 23S rRNA; thus, this result may explain the increase in the *rrn23* transcript of the *rh22-1* mutant shown in the qRT-PCR data. Consistent with the blots utilizing the b, c, and d probes, analysis of the *rh22* mutants with a 4.5S-specific probe (probe e) showed that the levels of the 3.2-kb precursor were increased and those of mature 4.5S rRNA were reduced (Fig. 4B). The amounts of mature 5S rRNA were also reduced in *rh22*, but accumulation of the 5S rRNA precursor was not detected (probe e). The precursor forms of the 23S and 4.5S rRNAs increased, whereas their mature forms decreased, indicating that processing of the 23-4.5S bicistronic RNA and its further maturation were affected in *rh22* mutants.

RH22 Associates with Precursors of the 50S Ribosomal Subunit

As described above, the 23S-4.5S precursor rRNA undergoes further processing to generate mature forms of 23S rRNA and 4.5S rRNA, and this processing is believed to occur on the ribosome (Keus et al., 1984; Strittmatter and Kössel, 1984; Leal-Klevezas et al., 2000). Because RH22 appears to be involved in the rRNA maturation process, we next tested whether RH22 was associated with chloroplast ribosomes. First, we performed an immunoblot analysis to examine whether RH22 cosedimented with chloroplast ribosomal particles when the stroma was subjected to a Suc gradient. During Suc gradient sedimentation, ribosomal particles migrate to the bottom of the gradient (Jenkins and Barkan, 2001). Thus, fractions 35 to 52, which were at the bottom of the Suc gradient, were selected for further analysis. The A_{260} profile of the gradient fractions revealed two peaks, one in fraction 43 and the other in fraction 48 (Fig. 5A), which corresponded to the mature 30S and 50S subunits, respectively, as shown by immunoblot analyses with RPS1, RPL4, and RPL32 antisera (Fig. 5B). Under these conditions, no effort was made to prevent ribosome runoff and dissociation, and the peak corresponding to the 70S ribosomes was not detected. RH22 was detected in fractions 46 to 51 (Fig. 5B). Nevertheless, no RH22 was found in fractions 46 and 47, and the RH22

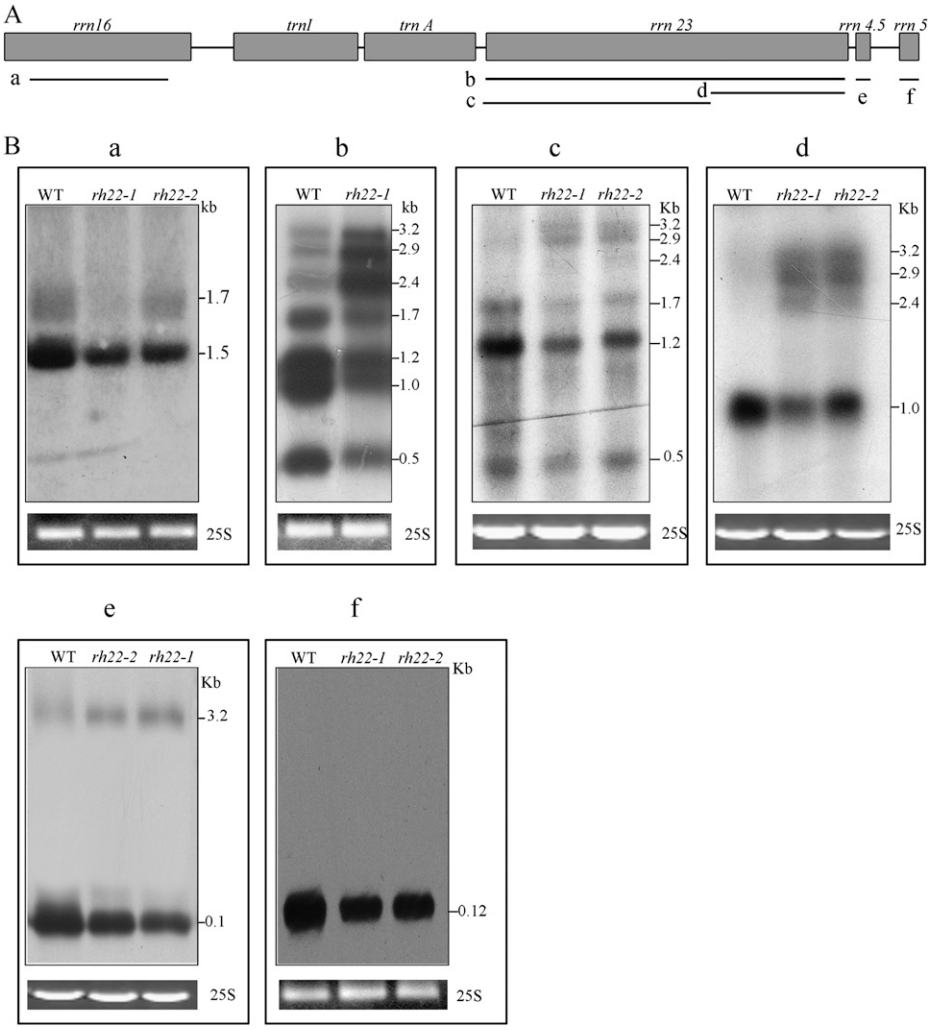

Figure 4. Expression and processing of chloroplast rRNA. A, Diagram of the chloroplast rRNA operon and the locations of the probes (a–f) used for the RNA gel-blot analysis. B, RNA gel analysis of 16S rRNA (probe a), 23S rRNA (probes b–d), 4.5S rRNA (probe e), and 5S rRNA (probe f). The sizes of the transcripts (in kb) are shown. The 25S rRNA stained with ethidium bromide is shown as a loading control. WT, Wild type.

peak did not correspond to the mature 50S subunit (Fig. 5B), showing that RH22 sediments more slowly than the mature 50S subunit.

The sedimentation behavior of RH22 in the Suc gradient raised the possibility that RH22 may be associated with 50S ribosomal subunit precursors. To test this possibility, RNAs that coimmunoprecipitated with the anti-RH22 antibody were analyzed by slot-blot hybridization using probes corresponding to the different regions of the *rrn* operon in chloroplasts (Fig. 5C). The *rrn23*, *rrn4.5*, and *rrn23-rrn4.5* intergenic spaces were also detected in substantial amounts in the precipitate, whereas *rrn16* and *rrn5* were not detected (Fig. 5C). This analysis suggests that RH22 may be bound to the 23S-4.5S precursors. Subsequently, an RNase-protection assay was used to map the 3′ end of the 23S rRNA that coimmunoprecipitated with RH22. Our results showed that the 23S-4.5S rRNA was enriched with respect to mature 23S rRNA in the RH22 immunoprecipitation pellets (Fig. 5D). The sedimentation behavior of RH22 and the coimmunoprecipitation of RH22 with the pre-23S rRNA indicate that RH22 is associated with an assembly intermediate of the 50S ribosomal subunit.

RH22 Interacts with the 50S Ribosomal Protein RPL24

The association of RH22 with the 50S ribosomal subunit may be mediated by the interaction of RH22 with the ribosomal protein. To address this possibility, we cloned RH22 lacking a signal peptide into the bait vector and then tested for its interaction with 59 distinct chloroplast ribosomal proteins that were fused to the GAL4-DNA-active domain in the prey vector. As shown in Figure 6A, RH22 specifically interacted with RPL24, one of the chloroplast 50S ribosome proteins. Coimmunoprecipitation analysis also showed that RPL24 was precipitated by an anti-RH22 antibody but not by preserum. As a control, we tested one of the 30S ribosome proteins, RPS1, and showed that it was not precipitated by the anti-RH22 antibody (Fig. 6B).

In *E. coli*, L24 and L4 are essential to generate the first intermediate during 50S assembly in vitro

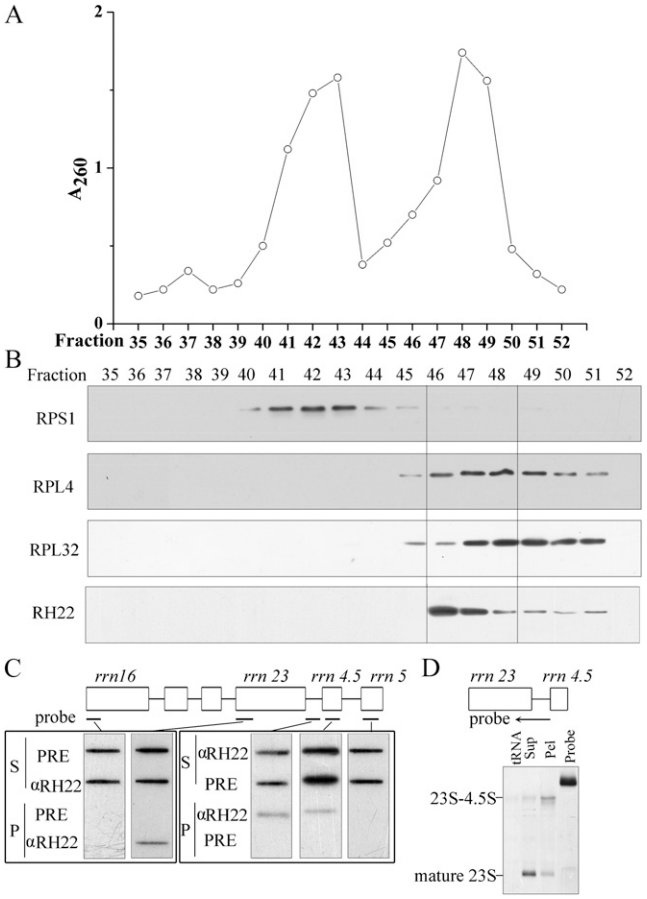

Figure 5. The association of RH22 with the precursor of the 50S ribosomal subunit. A, A_{260} profiles of fractions 35 to 52 from the Suc gradient sedimentation of stromal extracts. B, Immunoblot analyses of each fraction probed with antibodies against RPS1, RPL4, RPL32, and RH22. C, Coimmunoprecipitation of RH22 and rRNAs. The RNA from each immunoprecipitation (P) and supernatant (S) was applied to a nylon membrane with a slot-blot manifold and hybridized with probes as indicated. Immunoprecipitation with preimmune serum (PRE) was conducted as a negative control. D, RNase protection analysis of the 3′ end of the 23S rRNA in the immunoprecipitation pellet (Pel) and supernatant (Sup) samples. The probe is indicated below the diagram of the 23S-4.5S region of the *rrn* operon. The positions of the protected bands, corresponding to the mature rRNA and the 23S-4.5S precursor, are indicated.

(Trubetskoy et al., 2009). Because the chloroplast ribosome is similar to that of *E. coli*, we hypothesized that RH22 might interact with RPL4 as well. However, this interaction was not detected in our yeast two-hybrid assay (Fig. 6A). To further address this issue, we also performed a pull-down assay to investigate the interaction of RH22 with ribosomal proteins in vitro (Fig. 6C). Consistent with the yeast two-hybrid results, maltose-binding protein (MBP)-RH22 was able to pull down RPL24 but not RPL4. Based on these analyses, it is possible that RH22 interacts with RPL24, although an interaction between RH22 and RPL4 in vivo could not be excluded.

RH22 Can Bind to a 5′ Fragment of 23S rRNA

L24 is thought to be the first protein to bind 23S rRNA, thereby initiating the cooperative assembly process of the larger ribosome in *E. coli* (Egebjerg et al., 1987; Nierhaus, 1991; Tumminia et al., 1994). RH22 interacted with PRL24 in chloroplast ribosomes, raising the question of whether RH22 can bind to 23S rRNA. To answer this question, RH22 was generated from the recombinant protein by protease cleavage of the MBP moiety (Supplemental Fig. S5) and used for electrophoretic mobility shift assays (EMSAs) to detect its binding to RNA molecules. Two RNA oligonucleotides were used for the binding assay. One fragment was from the 5′ end of the 23S RNA (Oligo5), which encompassed the potential PRL24-binding site, as revealed by comparison with *E. coli* 23S rRNA; the other fragment was from the 3′ end of the 23S rRNA (Oligo3; Fig. 7A). EMSA revealed the formation of an RNA/protein complex when RH22 was incubated with Oligo5 but not with Oligo3 (Fig. 7B) under the conditions tested. The formation of the RNA/protein complex was increased with increasing protein concentrations (Fig. 7B). Complex formation was reduced when a 20- or 200-fold excess of unlabeled Oligo5 was added (Fig. 7C), whereas there was no change when unlabeled Oligo3 was added (Fig. 7D). This competition assay demonstrates that RH22 can specifically bind to Oligo5 RNA.

Polysomal Loading of mRNA in *rh22*

Abnormal ribosome assembly or rRNA processing may affect the polysomal loading of chloroplast mRNA (Barkan, 1993; Beligni and Mayfield, 2008), and defects in polysomal loading are usually observed in mutants with impaired chloroplast ribosome function (Fleischmann et al., 2011). The defects in rRNA accumulation observed in the *rh22* mutants prompted us to examine whether this characteristic affected the polysomal loading of chloroplast mRNAs. Extracts from wild-type or *rh22-1* seedlings were fractionated on 15% to 55% Suc density gradients and analyzed by RNA gel blot using probes targeting *rrn23*, *rrn16*, or the transcripts of several other chloroplast-encoded proteins (Fig. 8). In the wild-type plant, the 1.7-, 1.2-, 1.0-, and 0.5-kb components of the 23S rRNA were the major entities in the polysome fractions, but considerable amounts of 3.2-, 2.9-, and 2.4-kb precursors were also detected. In the *rh22-1* mutant, the polysome fractions contained all of these components, but the 3.2-, 2.9-, and 2.4-kb precursors were significantly enriched concomitant with the reduction of mature transcripts. The overall 16S rRNA polysome patterns of wild-type and *rh22-1* mutant plants were similar, but the levels of the 16S mature transcript were reduced in the *rh22-1* mutant. The lower levels of mature 23S and 16S rRNA components in the polysomal fractions indicated that the *rh22* chloroplasts contained fewer polysomes than the chloroplasts of wild-type

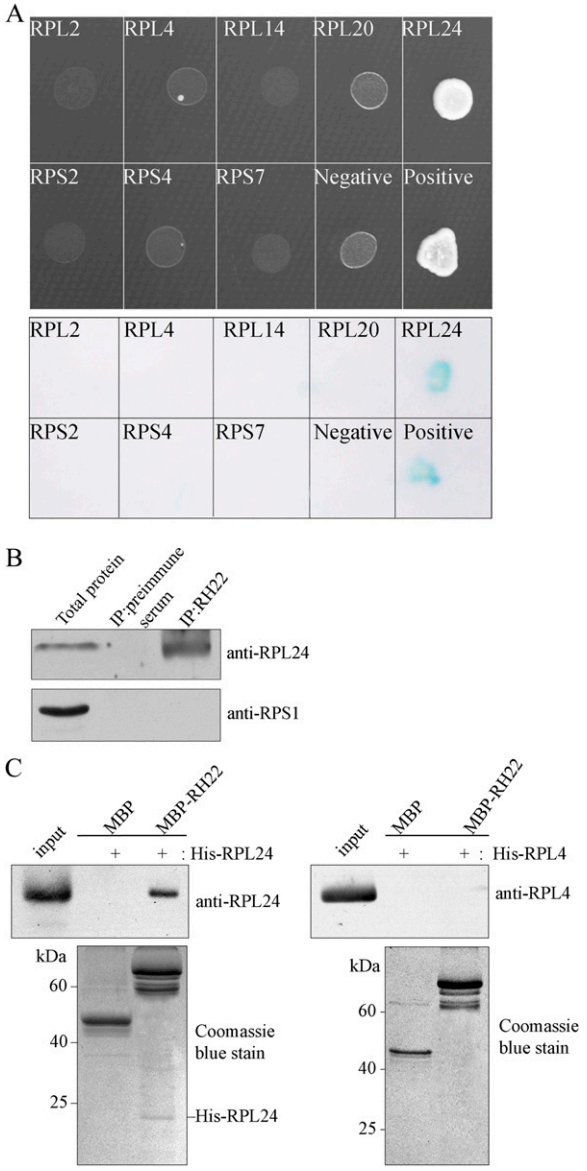

Figure 6. Interaction between RH22 and RPL24. A, Yeast two-hybrid analysis of RH22 interactions with ribosomal proteins. Yeast cells expressing RH22 and various ribosomal proteins are shown after growth at 30°C for 72 h on synthetic complete medium lacking Trp, Leu, and His and supplemented with 10 mM 3-amino-1,2,4-triazole. Yeast cells cotransformed with RH22 and the empty prey vector were used as negative controls, and those with pBD-WT and pAD-WT were used as positive controls. The results for several ribosomal proteins are indicated. The results for other ribosomal proteins that did not interact with RH22 are not shown. β-Galactosidase activity was visualized by transferring the cells to Whatman filters, permeabilizing them, and incubating them in the presence of 5-bromo-4-chloro-3-indolyl-β-D-galactopyranoside. B, Coimmunoprecipitation analysis of the interaction between RH22 and RPL24. Total protein extracts from Arabidopsis leaves were incubated with antibodies against RH22 or with a preimmune serum. Protein A-agarose beads were used to capture immunoprecipitates (IP), and the captured proteins were separated by SDS-PAGE, transferred onto nitrocellulose membranes, and detected by immunoblot analysis with anti-RPL24 antibody. The 30S ribosomal protein RPS1 was used as a control. C, Pull-down assay of RH22 protein interactions. MBP-tagged RH22 was used as the bait, and His-tagged RPL24 and RPL4 were used as prey. The purified recombinant proteins were bound to amylose resin, and the bound proteins were eluted and analyzed by immunoblot or staining. The position of His-RPL24 on the Coomassie-stained gel is indicated on the right.

plants. To determine whether RH22 is associated with polysomal fractions, proteins from each of the gradient fractions were analyzed by immunoblotting with anti-RH22 antibodies. RH22 was absent from the polysomal fractions but was easily detected in nonpolysomal regions of the gradient (Fig. 8).

The *rh22-1* seedlings exhibited reduced levels of chloroplast-encoded thylakoid proteins (Fig. 3); however, the polysomal loading of the corresponding transcripts (*psbA*, *psbB*, *psbD*, *psaA*, *petB*, and *atpB*) was not affected (Fig. 8). Because the polysomal loading of *rbcL*, which encodes the large subunit of Rubisco, has been shown to be more sensitive to mild defects in chloroplast translation than *psbA* (Rogalski et al., 2008), its polysomal loading was also investigated (Fig. 8). No substantial change in polysomal loading of *rbcL* was detected in *rh22-1*, and similar results were observed in *rnr1* and *rh39*, two other ribosomal biogenesis mutants (Bollenbach et al., 2005; Nishimura et al., 2010). Defects in the initiation step of chloroplast translation usually lead to the alteration of ribosomes associated with mRNAs (Barkan, 1993). There was no significant difference in the polysomal loading of these transcripts between the wild type and *rh22-1*, suggesting that the initiation step of the chloroplast translation is not affected. Instead, other translation steps might be impaired in this mutant.

DISCUSSION

The components of chloroplast ribosomes have been determined in spinach (*Spinacia oleracea*; Yamaguchi and Subramanian, 2000, 2003; Yamaguchi et al., 2000), barley (*Hordeum vulgare*; Maki et al., 2000), and *Chlamydomonas reinhardtii* (Yamaguchi et al., 2003). However, the mechanism by which this discrete set of components assembles into this large, functional complex and coordinates with rRNA molecules still remains largely unknown. In this study, we reported the functional characterization of the chloroplast DEAD RNA helicase RH22 from Arabidopsis and investigated its roles in ribosomal biogenesis.

RH22 Is Involved in the Biogenesis of the 50S Ribosome

The maturation of chloroplast rRNAs involves multiple exonucleolytic and endonucleolytic events, similar to the process in bacteria (Strittmatter and Kössel, 1984). Indeed, the components of the enzymatic rRNA metabolism machinery have been implicated in the maturation of rRNA transcripts. RNR1, an RNase R

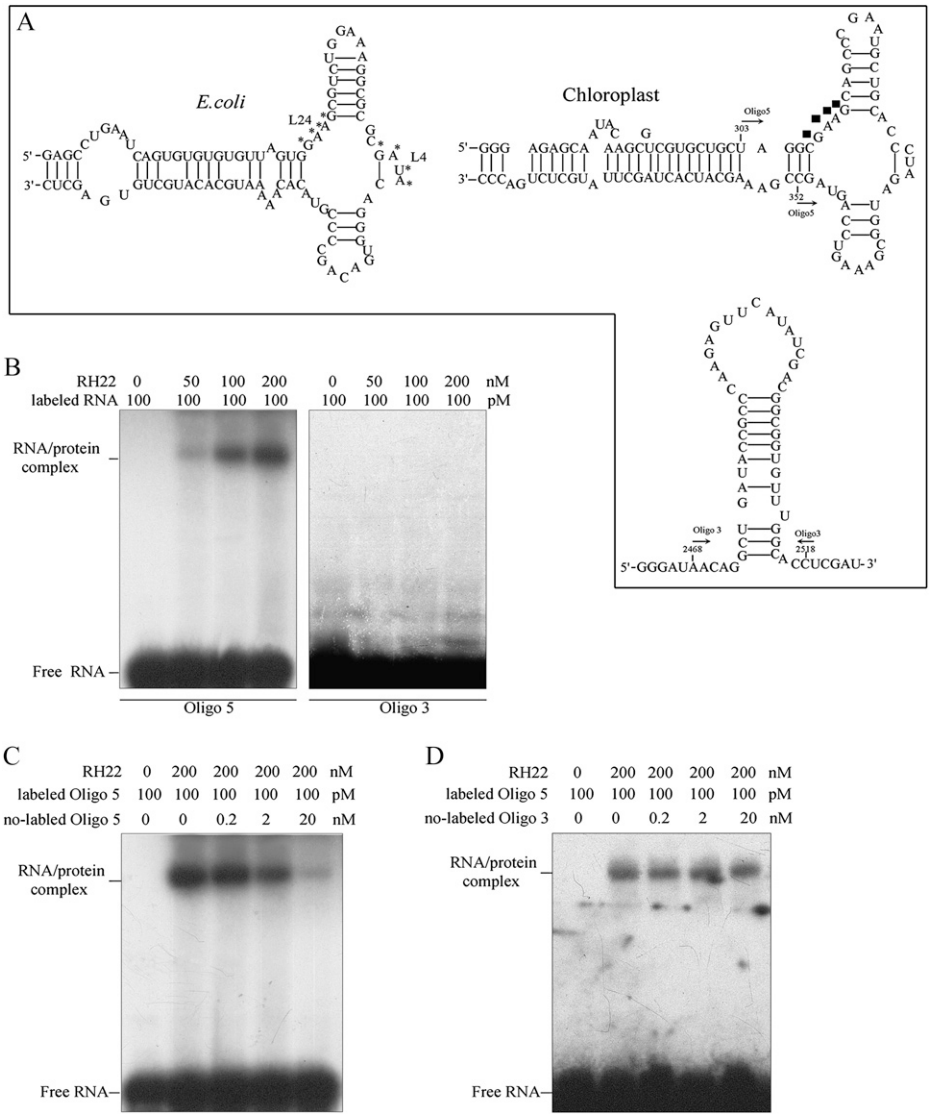

Figure 7. RH22 binds to the 5′ fragment of the 23S rRNA in vitro. A, Comparison of the secondary structures of the 23S rRNA fragments that contain L24-binding sites in *E. coli* and the Arabidopsis chloroplast and the oligoribonucleotide RNA that was used for the EMSA. The nucleotides of *E. coli* that are directly bound to L24 and L4 are indicated by asterisks (Stelzl and Nierhaus, 2001). The putative L24-binding nucleotides in the Arabidopsis chloroplast sequence are shown as squares. The positions of the two oligoribonucleotides, Oligo5 (right of top panel; 303–352) and Oligo3 (bottom panel; 2,468–2,518 of 23S rRNA), are indicated. Oligo3 is localized in the peptidyltransferase region of the 23S rRNA. B, EMSA demonstrating the binding of RH22 to a 23S rRNA. The RNA oligonucleotides used are shown in A. The substrate (100 pM) was mixed with increasing concentrations of RH22 (0, 50, 100, and 200 nM). The positions of the free RNA and the protein/RNA complex are indicated. C, Competition assay with unlabeled Oligo5. As indicated at the top, a 2-, 20-, and 200-fold molar excess of unlabeled Oligo5 RNA was introduced as a competitor into the reaction mixtures (lanes 3–5 from the left). D, The competition assay with unlabeled Oligo3. The competition was similar to that in C.

homolog, acts as a 3′-to-5′ exoribonuclease and is involved in trimming the 3′ ends of 23S, 16S, and 5S rRNAs (Bollenbach et al., 2005). The Arabidopsis *rnr1* mutant is impaired in the processing of 23S-4.5S precursors and has a defect that affects the accumulation of mature rRNAs (Bollenbach et al., 2005). The chloroplast polynucleotide phosphorylase (PNPase) is a 3′-to-5′ exoribonuclease that mediates efficient 3′ end trimming of chloroplast mRNAs and 23S rRNA via its phosphorolytic activity (Walter et al., 2002). 23S rRNA with 3′ extensions accumulates in Arabidopsis plants with reduced or absent chloroplast PNPase (Walter et al., 2002; Marchive et al., 2009; Germain et al., 2011). CSP41a/b, two ribosome-associated endonucleases, can alter the balance between 23S precursor and mature rRNA in vitro, and these endonucleases likely act in the final steps of 23S rRNA maturation (Beligni and Mayfield, 2008). No RNase activity has been documented for any DEAD RNA helicase thus far; therefore, it is unlikely that RH22 functions as an RNase. However, DEAD RNA helicases may act as auxiliary and accessory proteins to facilitate rRNA metabolism in combination with RNases. For instance, the DEAD RNA helicase RhlB is present in the *E. coli* degradosome (Coburn et al., 1999). The chloroplast DEAD RNA helicase RH39 has been suggested to be involved in the introduction of the hidden break into the 23S rRNA in combination with an unknown endoRNase (Nishimura et al., 2010). RH22, similar to RH39, may be implicated in the regulation of chloroplast rRNA maturation. However, the behavior of RH22 is distinct from that of RH39, as the contents of one mature form of 23S rRNA, the 0.5-kb fragment, were not affected in *rh39* mutant plants (Nishimura et al., 2010).

In *E. coli*, ribosome assembly and pre-rRNA processing/maturation are intimately linked (Charollais et al., 2003; Granneman and Baserga, 2005). For this reason, processing defects are frequently found in mutants with primary lesions in ribosome assembly

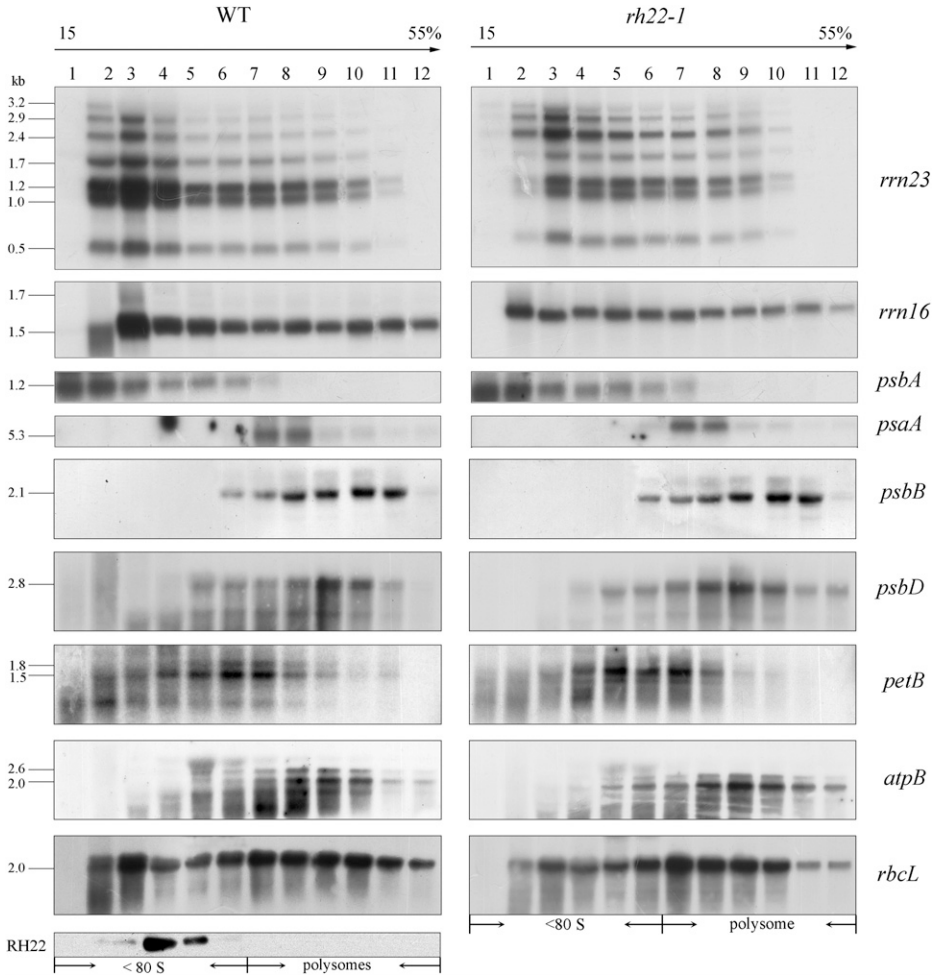

Figure 8. Polysomal loading in *rh22* and wild-type (WT) plants. Twelve fractions of equal volume were collected from top to bottom of 15% to 55% Suc gradients, and equal proportions of the RNA purified from each fraction were analyzed by gel-blot hybridization with the probes indicated at the right of each panel. The positions of the ribosome (less than 80S) and the polysomal fractions were determined by running puromycin-treated samples in parallel with the experimental samples, as indicated at the bottom. The sedimentation of RH22 in the wild-type extracts was followed by an immunoblot analysis of the proteins from the same gradient fractions.

and/or function. Thus, defects in rRNA processing or maturation could be caused by defects in the RNA processing itself or in ribosome assembly (Granneman and Baserga, 2005). Although the ribosomal assembly process in chloroplasts is not well understood, the principles governing *E. coli* ribosome assembly may be applicable to chloroplast ribosome assembly as well. Therefore, the aberrant processing and maturation of chloroplast rRNA in some mutants may result from a defect in ribosomal assembly. For example, in the *ppr4* mutant, the 16S rRNA-processing defect might be a consequence of incomplete 30S subunit assembly, which in turn may result from an impairment of RPS12 synthesis (Schmitz-Linneweber et al., 2006).

In this study, Suc gradient analyses and RNA coimmunoprecipitation assays produced strong evidence that RH22 is associated with the pre-50S subunit, which suggests that RH22 is involved in 50S ribosomal subunit assembly (Fig. 5). Thus, we propose that the rRNA maturation defect in the *rh22* mutants may be caused by defects in the assembly of the 50S ribosomal subunits rather than by defective processing per se. Indeed, further analysis showed that RH22 could specifically bind to a fragment of domain I of 23S rRNA (Fig. 7), around which no cleavage sites for 23S rRNA processing exist. Various steps in rRNA processing depend on ribosome assembly. In *E. coli* cell extracts, pre-23S rRNA in free ribosomes did not mature; however, this RNA was efficiently processed in polysomes, which suggests that formation of the polysomal complex is required for rRNA processing (Srivastava and Schlessinger, 1988). Similarly, the formation of a functional translation apparatus may be required for the normal maturation of chloroplast rRNAs (Barkan, 1993). However, RH22 does not seem to be associated with the polysomal fractions (Fig. 8) and is thus unlikely to be involved in polysome assembly.

The *rh22* mutants also showed a reduction in the mature forms of 16S rRNA, whereas an accumulation of the precursor rRNA was not observed (Fig. 4). The decrease in mature 16S rRNA in *rh22* appeared to represent an indirect consequence of the defect in 50S subunit biogenesis, because RH22 was not found to be associated with the 30S particle (Figs. 5 and 6). A similar phenomenon has been observed in the *E. coli srmB* mutant. In *srmB*, assembly of the 50S ribosomal subunit is affected, but incorporation of the 30S subunit into the 70S ribosome was also impaired, delaying the maturation of 16S rRNA (Charollais et al., 2003). How-

ever, Tiller et al. (2011) analyzed the rRNA-processing defects of Arabidopsis ribosomal mutants in RPS17, RPL24, and five plastid-specific ribosomal proteins. They found that defects in these mutants seem to be mainly specific to either the large or small subunit of the chloroplast ribosome (Tiller et al., 2011), in contrast to our results. Another possible reason for the decrease of mature 16S rRNA in *rh22* is that RH22 has other functions in addition to its role in ribosome assembly. RH22 may be involved in the regulation of other processes associated with rRNA gene expression, such as rRNA transcription or the stabilization of rRNA transcripts. For example, CSP41a/b has roles not only in the assembly of the 50S subunit of the chloroplast ribosome but also in the activation of chloroplast-encoded RNA polymerase (Beligni and Mayfield, 2008; Bollenbach et al., 2009).

Potential Roles of RH22 in Ribosomal Assembly

Using yeast two-hybrid analysis and coimmunoprecipitation assays, we showed that RH22 can interact with the L24 protein of the chloroplast 50S ribosomal subunit (Fig. 6). Using EMSA analysis, we also showed that RH22 can bind to a 5′ fragment of 23S rRNA that belongs to domain I of the 23S rRNA and includes putative PRL24-binding sites (Fig. 7). An RNA/protein complex containing RH22 appears to be formed during assembly of the 50S ribosomal subunit in chloroplasts. A similar RNA/protein complex involving SrmB, the DEAD RNA helicase involved in 50S assembly, was identified in *E. coli*; this complex comprises the ribosomal proteins L24 and L4 and a small 23S rRNA fragment that encompasses their binding sites (Trubetskoy et al., 2009). Phylogenetic analysis of the DEAD RNA helicase proteins from bacteria and chloroplasts with the Phylogeny.fr program online (for details, see Supplemental References S1) indicated that RH22, RH39, RH50, and SrmB are grouped into one cluster and that RH3, RH26, and other bacterial DEAD-box proteins are grouped into another cluster (Supplemental Fig. S6). This analysis suggested that RH22 may have evolved from the bacterial SrmB protein. The reconstitution assay suggested that the L24 and L4 proteins might interact directly with SrmB via protein-protein contacts (Trubetskoy et al., 2009). Consistent with this hypothesis, we identified chloroplast RPL24 as an interaction partner for RH22, suggesting that the action of RH22 is similar to that of SrmB in *E. coli*. Based on the data presented here, we could not determine whether RPL4 interacts with RH22 in vivo, but no interaction between RH22 and L4 protein was detected in either the yeast two-hybrid or pull-down assay. However, if RPL4 is truly not a partner of RH22, this would indicate that the functional property of RH22 is not identical to that of SrmB. In *E. coli*, L4, L24, and domain I are presumably among the first components of the 50S subunit to associate with one another, and SrmB is involved in the formation of this complex (Trubetskoy et al., 2009). Domain I of the 23S rRNA in chloroplasts is very similar to that in *E. coli*, although it lacks helix 8 and contains additional sequence between helices 13 and 14 (Branlant et al., 1981; Edwards and Kössel, 1981; Harris et al., 1994). The binding sites of L24 and L4 in the *E. coli* 23S rRNA are thought to be in the internal loops that are bordered by helices 18, 19, and 20 in domain I (Fig. 7A; Stelzl and Nierhaus, 2001). The chloroplast 23S rRNA has a similar helical structure in domain I (Fig. 8A). However, putative binding sites for RPL24 (GAAG), but not RPL4, were found in chloroplast 23S rRNA (Fig. 7A). This structural difference in the 23S rRNA molecules of *E. coli* and chloroplasts suggests that chloroplast RPL4 may not bind to this region or that it binds to this region in a manner distinct from that in *E. coli*. It is likely that the functions and activities of DEAD RNA helicases may coevolve with rRNA structure in the context of ribosome function.

If RH22, PRL24, and the 5′ end of 23S rRNA form a protein/RNA complex, and this complex is involved in the early assembly of the 50S subunit, how does RH22 participate in this process? Many rRNA-rRNA and rRNA-protein interactions certainly occur during 23S RNA processing and its assembly with 50S ribosomal proteins. These interactions cause extensive structural rearrangements that ultimately lead to formation of the functional ribosomal complex. The association of RH22 with the 5′ end of the 23S RNA may facilitate its interaction with RPL24 and the initiation of 50S ribosome assembly. The helicase activity of RH22 may unwind and/or rearrange the structure of the 23S precursor rRNA to allow it to contact PRL24. It has been reported that DpbA, an ATP-dependent helicase in *E. coli*, was able to bind to hairpin 92 of 23S rRNA to promote a conformational change of the peptidyl transferase center of 23S rRNA and affect its association with several ribosomal proteins (Sharpe Elles et al., 2009). Alternatively, RH22 may simply clamp its RNA-binding track on the 23S rRNA to transiently stabilize the RNA structure and maintain its structure to facilitate the kinetics of ribosome assembly. In eukaryotes, the DEAD-box initiation factor 4AIII can interact with the phosphate-ribose backbone of six consecutive nucleotides and prevent part of the bound RNA from forming a duplex with another strand, which is required for the formation of a multiprotein exon junction complex (Andersen et al., 2006).

MATERIALS AND METHODS

Plant Materials and Growth Conditions

Wild-type and mutant Arabidopsis (*Arabidopsis thaliana* ecotype Columbia) plants were grown in soil under short-day conditions (10-h-light/14-h-dark cycles) with a photon flux density of 120 μmol m^{-2} s^{-1} at 22°C. To ensure synchronized germination, the seeds were incubated in darkness for 48 h at 4°C before sowing. For growth on agar plates, the seeds were surface sterilized and sown on Murashige and Skoog medium containing 2% Suc. Three *rh22* mutant lines, Salk_032399 (*rh22-1*), Salk_065388C (*rh22-2*), and CS856759 (*rh22-3*), were obtained from the ABRC and identified using PCR analysis according to the methods of Alonso et al. (2003) and Woody et al. (2007).

Chlorophyll Fluorescence Measurements

Chlorophyll fluorescence measurements were performed using CF Imager (Technologica) as described in the manufacturer's instructions. Before each measurement, leaves were dark adapted for 10 min. The minimum fluorescence yield (F_o) was measured under measuring light (650 nm) with very low intensity (0.8 μmol m^{-2} s^{-1}). A saturating pulse of white light (3,000 μmol m^{-2} s^{-1} for 1 s) was applied to estimate the maximum fluorescence yield (F_m). The maximal photochemical efficiency of PSII was calculated from the ratio of F_v to F_m [$F_v/F_m = (F_m - F_o)/F_m$]. Values of F_o and F_m were averaged to improve the signal-to-noise ratio. Image data acquired in each experiment were normalized to a false-color scale, with arbitrarily assigned extreme values of 0.1 (lowest) and 0.8 (highest). This resulted in the highest and lowest F_v/F_m values being represented by the red and blue extremes of the color scale, respectively.

GFP Assays

The coding sequences of *RH22* were amplified by RT-PCR using primers 5′-GTCGACAGTGAGCTAATGAAGAGAGAGAC-3′ and 5′-CCATGGCTCGGCATAAACGAGATTGTATT-3′. The PCR products were then cloned into *Sal*I/*Nco*I sites of the transient expression vector pUC18-35s-sGFP, which contained the mGFP5 coding sequence under the control of the cauliflower mosaic virus 35S promoter, to generate a RH22 fusion protein with GFP in the C terminus. Similarly, the fragments containing the transit peptide (1–81 amino acids) of the small subunit of ribulose bisphosphate carboxylase were amplified using the primer pair 5′-CACGTCGACAAACCTCAGTCACACAAAGAG-3′ and 5′-TCCATGGATTCGGAATCGGTAAGGTCAGG-3′, which were subcloned into this vector and used as the chloroplast localization control. The resulting constructs and the negative control vector without additional coding sequence were transfected into Arabidopsis mesophyll protoplasts according to the method described by Kovtun et al. (2000). Fluorescence analysis was performed on a LSM 510 META confocal laser-scanning system (Zeiss).

Protein Isolation and Immunoblotting

Protein of thylakoid membrane was isolated essentially as described by Zhang et al. (1999). Briefly, 0.1 g of Arabidopsis leaves was homogenized in an ice-cold extraction buffer (400 mM Suc, 50 mM HEPES-KOH, pH 7.8, 10 mM NaCl, and 2 mM $MgCl_2$), filtered through two layers of cheesecloth, and centrifuged at 5,000*g* for 10 min. The thylakoid pellets were resuspended in the isolation buffer and then centrifuged at 5,000*g* for 10 min. The thylakoids were finally suspended in isolation buffer, and their protein levels were quantified using the Dc protein assay kit (Bio-Rad) according to the manufacturer's instructions. The leaf total protein was isolated according to the method of Chi et al. (2010). The proteins resolved by SDS-PAGE were blotted onto nitrocellulose membranes and incubated with specific antibodies, and the signals were detected using the enhanced chemiluminescence method.

RNA Preparation and RT-PCR Analysis

Total leaf RNA was purified from Arabidopsis seedlings using Trizol reagent (Invitrogen). Total RNA (500 ng) was used to generate the first-strand cDNA in a 50-μL reaction with the SuperScript II cDNA synthesis system (Invitrogen) according to the manufacturer's instructions. The resulting cDNA samples were then used for PCR analysis. The PCR primers for detection of *RH22* expression (in Fig. 2) were FP (5′-ATGATTCTCTCACGCTCTGTCTC-3′) and RP (5′-TTAATATCTCACAGCTTGAGGCTC-3′). The specific primers of chloroplast genes for qPCR were adopted from Chateigner-Boutin et al. (2008). The qRT-PCR was performed using Mx3000P (Stratagene) with SYBR Green I (Invitrogen) according to the manufacturers' protocols. The amplification of *ELONGATION FACTOR1-α* was used as an internal control for normalization.

RNA-Blot Analysis

Five micrograms of total RNA from wild-type and *rh22* seedlings was separated on a 1.2% to 3.0% (w/v) agarose-formaldehyde gel, blotted to a positively charged nylon membrane by capillary blotting, and fixed by cross-linking. Hybridization was performed with ^{32}P-labeled probes in 5× SSC, 5× Denhardt's solution, and 0.5% SDS at 65°C overnight. The membranes were washed twice in 2× SSC, 0.1% SDS and once in 1× SSC, 0.1% SDS at 65°C.

Hybridization probes were prepared from the PCR amplification fragments of the following chloroplast genes of Arabidopsis (GenBank accession no. AP000423): *psbA* (position 293–1,036), *psbB* (position 72,671–73,185), *psbD* (position 32,908–33,576), *atpB* (position 52,543–53,286), *psaA* (position 40,193–40,754), *petA* (position 61,657–62,420), *rrn16* (position 101,050–102,482), *rrn23* (5′ end; position 104,691–106,691), *rrn23* (3′ end; position 106,692–107,500), *rrn4.5* (position 107,599–107,701), and *rrn5* (position 130,580–130,700).

Expression of Recombinant Proteins and Antibody Production

The DNA sequence of mature RH22 was subcloned into the expression vector pMAL-c4x (New England Biolabs) to produce MBP fusions. The MBP-RH22 fusion protein was expressed in *Escherichia coli* BL21 (DE3) cells. Induction, cell lysis, and purification of the fusion protein using amylose affinity chromatography were performed according to the manufacturer's protocol. The fusion protein was cleaved with the specific protease factor Xa, dialyzed with 20 mM Tris-HCl and 25 mM NaCl, pH 8.0, and fractionated on a 1- × 10-cm DEAE-Sepharose chromatography column (GE Life Sciences) according to the manufacturer's protocol. The fractions containing proteins were determined by measuring A_{280} and analyzed by SDS-PAGE and Coomassie blue staining. The fractions containing the RH22 protein free of MBP were pooled and concentrated. Mature RPL24 and RPL4 with an N-terminal 6× His tag were expressed from the pET28a vector (Novagen), and the recombination protein was purified with the nickel-nitrilotriacetic acid agarose resin (Qiagen). The MBP-RH22 and His-RPL24 fusion proteins were used to generate polyclonal antibodies from rabbits. The antibodies of RPS1, RPL4, and RPL32 were supplied by Uniplastomic of France (http://www.uniplastomic.com/).

Suc Gradient Sedimentation Analysis

The isolation of intact chloroplasts was performed as described previously (Barkan, 1998). The stroma was prepared by hypotonic lysis of purified chloroplasts and used for Suc gradient sedimentation analysis as described by Jenkins and Barkan (2001). Briefly, intact chloroplasts underwent osmotic lysis in 30 mM HEPES-KOH, pH 8, 60 mM KOAc, 10 mM Mg$(OAc)_2$, 2 mM dithiothreitol (DTT), and a protease inhibitor cocktail (2 mg mL^{-1} aprotinin, 2 mg mL^{-1} leupeptin, 1 mg mL^{-1} pepstatin, and 1 mM phenylmethylsulfonyl fluoride) with repeated vortexing and incubation on ice for 30 min. The stromal fraction was obtained from lysed plastids by centrifugation at 29,000 rpm for 30 min at 4°C. A layer of 200 μL of stroma extract (about 10 mg mL^{-1}) was placed on the top of 10% to 40% linear Suc gradients prepared in 30 mM HEPES-KOH, pH 8.0, 10 mM Mg$(OAc)_2$, 150 mM KOAc, and 5 mM DTT. Gradients were centrifuged in a Beckman SW55.1 rotor at 48,000 rpm for 4 h at 4°C. The gradients were fractionated by carefully pipetting from the top of the gradient, and 100 μL per fraction was collected for further analysis.

Pull Down and Coimmunoprecipitation of Proteins and RNA

The pull-down assay was performed according to the method described by Chi et al. (2010) with modifications. MBP only and MBP-RH22 fusion proteins were mixed with testing proteins (His-RPL24 and His-RPL4) in 20 mM Tris-HCl, pH 7.4, 200 mM NaCl, and 1 mM EDTA and incubated for 2 h at 4°C. Afterward, unbound proteins were removed by washing three times with 20 mM Tris-HCl, pH 7.4, 200 mM NaCl, 1 mM EDTA, and 0.5% Nonidet P-40. The bound proteins were eluted and separated by SDS-PAGE followed by immunoblot analysis or Coomassie blue staining.

Protein coimmunoprecipitations were performed as described previously (Chi et al., 2010). Wild-type Arabidopsis seedling leaves (0.05 g) were homogenized with 1% (w/v) dodecyl β-D-maltoside in 100 μL of phosphate-buffered saline buffer (pH 7.4) at 0°C and centrifuged at 12,000*g* for 10 min. The supernatant was incubated with the anti-RH22 antibodies coupled covalently to Protein A-Sepharose beads for 4 h at 4°C. After the Sepharose beads were washed three times with phosphate-buffered saline buffer containing 0.1% Nonidet P-40, the precipitated proteins were dissociated in SDS sample buffer by heating at 95°C for 5 min. The precipitated proteins were separated by SDS-PAGE and immunobloted with anti-RPL24 and anti-RPS1 antibodies.

RNA coimmunoprecipitations were performed as described by Barkan (2009). Briefly, RNA was recovered from the precipitated fractions in the presence of 1% SDS, 0.05 μg μL^{-1} yeast tRNA, and 5 mM EDTA. The RNA was isolated by phenol-chloroform isoamyl extraction and precipitated with 3 volumes of ethanol. RNAs from the supernatant fractions were extracted as the controls. RNA samples were transferred to a nylon membrane using a slot-blotting apparatus (Bio-Dot SF; Bio-Rad). Subsequently, the membranes were hybridized with radiolabeled DNA probes.

For the RNase-protection assay of the RNA samples, α-^{32}P-radiolabeled RNA probes were synthesized using the MAXIscript kit (Ambion) with templates amplified from Arabidopsis total DNA according to the manufacturer's instructions. The hybridization, the RNase digestion of the unhybridized RNA, and the separation and detection of protected fragments were performed using the RPAIII kit (Ambion).

Yeast Two-Hybrid Analysis

The protein interactions were detected using the HybriZAP-2.1 two-hybrid system (Stratagene) as described previously (Chi et al., 2010). The cDNA corresponding to the RH22 protein lacking the N-terminal 58 amino acids of the signal peptide amplified using PCR was cloned into the *Srf*I and *Sal*I sites of the pBD-GAL4 Cam vector and used as the bait. The primers used were as follows: sense (5′-GCCCGGGCGCGTCTGCTACTGAAGCAGAAGTC-3′) and antisense (5′-GTCGACATATCTCACAGCTTGAGGCTCCTCT-3′). The cDNAs corresponding to mature ribosomal proteins were amplified using PCR and cloned into the pAD-GAL4-2.1 vector as the prey. The information for all of the ribosomal proteins was obtained from PPDB, a plant proteome database for Arabidopsis and maize (*Zea mays*) at Cornell University (Sun et al., 2009). Protein interactions were determined by growing yeast transformants on selective medium plates (without Trp, Leu, and His but containing 10 mM 3-amino-1,2,4-triazole). The β-galactosidase activities were measured using the 5-bromo-4-chloro-3-indolyl-β-D-galactopyranoside filter assay according to the manufacturer's instructions.

EMSAs

The two oligoribonucleotides used for EMSA were synthesized by Takara, and their sequences were as follows: Oligo5 (5′-UAGGCGAAGCAGCCCGAAUGCUGCACCCUAGAUGGCGAAAGUCCAGUAGUAGC-3′; 303–352 of *rrn23*) and Oligo3 (5′-AACAGGCUGAUACCGCCCAAGAGUUCAUAUCGACGGCGGUGUUUGGCACC-3′; 2,468–2,518 of *rrn23*). The synthetic oligoribonucleotides were 5′ end labeled with [γ^{32}P]ATP and T4 polynucleotide kinase and purified by ethanol precipitation. The binding reaction mixture contained 50 mM Tris-HCl, pH 7.5, 150 mM NaCl, 2 mM DTT, 5% glycerol, 0.1 mg mL^{-1} bovine serum albumin, 0.5 mg mL^{-1} heparin, and 5 units of RNasin. The concentrations of RNA and RH22 protein are indicated in Figure 7. After incubation for 30 min at 25°C, the samples were resolved on a 4% Tris-borate gel in 0.25× Tris-borate buffer, dried, and subjected to autoradiography.

Polysome Analysis

Polysomes were isolated according to the method of Barkan (1993). Two-tenths of 1 g of leaf tissues was homogenized in 1 mL of polysome extraction buffer (0.2 M Tris-HCl, pH 9, 0.2 M KCl, 35 mM $MgCl_2$, 25 mM EGTA, 0.2 M Suc, 1% Triton X-100, 2% polyoxyethylene-10-tridecyl ether, 0.5 mg mL^{-1} heparin, 100 mM β-mercaptoethanol, 100 μg mL^{-1} chloramphenicol, and 25 μg mL^{-1} cycloheximide). After incubation for 10 min on ice, the nuclei and the insoluble materials were removed by centrifugation at 12,000 rpm for 5 min at 4°C. Sodium deoxycholate was added to the supernatant at a concentration of 0.5%, and the mixture was then placed on ice for 5 min. The remaining insoluble materials were removed by centrifuging at 12,000 rpm for 15 min at 4°C. The supernatants (0.4 mL) were layered on 4.4 mL of a 15% to 55% Suc density gradient. Samples were centrifuged in a SW55Ti rotor (Beckman) at 45,000 rpm for 65 min at 4°C. After centrifugation, 12 fractions (410 μL each) were collected, and the RNA was isolated from each faction and used for RNA gel-blot analysis as described above.

Sequence data from this article can be found in the GenBank/EMBL data libraries under accession numbers RH22(At1g59990).

Supplemental Data

The following materials are available in the online version of this article.

Supplemental Figure S1. Transmission electron microscopic images of chloroplasts in 10-d-old leaves from wild-type and *rh22* mutant seedlings.

Supplemental Figure S2. Microscopy of the developing embryos in opened developing siliques of wild-type and heterozygous *rh22-3/RH22* plants.

Supplemental Figure S3. RNA gel-blot analysis of the levels of chloroplast-encoded gene transcripts in wild-type and *rh22-1* plants.

Supplemental Figure S4. qRT-PCR assay of chloroplast gene expression in wild-type and *rh22-1* plants.

Supplemental Figure S5. Expression and purification of RH22 protein.

Supplemental Figure S6. Phylogenetic analysis of DEAD RNA helicase proteins from the chloroplast and *E. coli*.

Supplemental Materials and Methods.

Supplemental References S1. The phylogeny.fr program.

ACKNOWLEDGMENTS

We are especially grateful to Dr. Alice Barkan for helpful instructions with the preparation of the Suc gradient. We also thank the ABRC for the *rh22* mutant lines.

Received September 8, 2011; accepted December 12, 2011; published December 14, 2011.

LITERATURE CITED

Alonso JM, Stepanova AN, Leisse TJ, Kim CJ, Chen H, Shinn P, Stevenson DK, Zimmerman J, Barajas P, Cheuk R, et al (2003) Genome-wide insertional mutagenesis of *Arabidopsis thaliana*. Science **301:** 653–657

Andersen CB, Ballut L, Johansen JS, Chamieh H, Nielsen KH, Oliveira CL, Pedersen JS, Séraphin B, Le Hir H, Andersen GR (2006) Structure of the exon junction core complex with a trapped DEAD-box ATPase bound to RNA. Science **313:** 1968–1972

Aubourg S, Kreis M, Lecharny A (1999) The DEAD box RNA helicase family in *Arabidopsis thaliana*. Nucleic Acids Res **27:** 628–636

Ban N, Nissen P, Hansen J, Moore PB, Steitz TA (2000) The complete atomic structure of the large ribosomal subunit at 2.4 A resolution. Science **289:** 905–920

Barkan A (1993) Nuclear mutants of maize with defects in chloroplast polysome assembly have altered chloroplast RNA metabolism. Plant Cell **5:** 389–402

Barkan A (1998) Approaches to investigating nuclear genes that function in chloroplast biogenesis in land plants. Methods Enzymol **297:** 38–57

Barkan A (2009) Genome-wide analysis of RNA-protein interactions in plants. Methods Mol Biol **553:** 13–37

Beick S, Schmitz-Linneweber C, Williams-Carrier R, Jensen B, Barkan A (2008) The pentatricopeptide repeat protein PPR5 stabilizes a specific tRNA precursor in maize chloroplasts. Mol Cell Biol **28:** 5337–5347

Beligni MV, Mayfield SP (2008) *Arabidopsis thaliana* mutants reveal a role for CSP41a and CSP41b, two ribosome-associated endonucleases, in chloroplast ribosomal RNA metabolism. Plant Mol Biol **67:** 389–401

Bellaoui M, Keddie JS, Gruissem W (2003) DCL is a plant-specific protein required for plastid ribosomal RNA processing and embryo development. Plant Mol Biol **53:** 531–543

Bisanz C, Bégot L, Carol P, Perez P, Bligny M, Pesey H, Gallois JL, Lerbs-Mache S, Mache R (2003) The *Arabidopsis* nuclear *DAL* gene encodes a chloroplast protein which is required for the maturation of the plastid ribosomal RNAs and is essential for chloroplast differentiation. Plant Mol Biol **51:** 651–663

Bollenbach TJ, Lange H, Gutierrez R, Erhardt M, Stern DB, Gagliardi D (2005) RNR1, a 3′-5′ exoribonuclease belonging to the RNR superfamily, catalyzes 3′ maturation of chloroplast ribosomal RNAs in *Arabidopsis thaliana*. Nucleic Acids Res **33:** 2751–2763

Bollenbach TJ, Sharwood RE, Gutierrez R, Lerbs-Mache S, Stern DB (2009) The RNA-binding proteins CSP41a and CSP41b may regulate transcription and translation of chloroplast-encoded RNAs in *Arabidopsis*. Plant Mol Biol **69:** 541–552

Branlant C, Krol A, Machatt MA, Pouyet J, Ebel JP, Edwards K, Kössel H (1981) Primary and secondary structures of *Escherichia coli* MRE 600 23S ribosomal RNA: comparison with models of secondary structure for maize chloroplast 23S rRNA and for large portions of mouse and human 16S mitochondrial rRNAs. Nucleic Acids Res **9:** 4303–4324

Caruthers JM, McKay DB (2002) Helicase structure and mechanism. Curr Opin Struct Biol **12:** 123–133

Charollais J, Dreyfus M, Iost I (2004) CsdA, a cold-shock RNA helicase from *Escherichia coli*, is involved in the biogenesis of 50S ribosomal subunit. Nucleic Acids Res **32:** 2751–2759

Charollais J, Pflieger D, Vinh J, Dreyfus M, Iost I (2003) The DEAD-box RNA helicase SrmB is involved in the assembly of 50S ribosomal subunits in *Escherichia coli*. Mol Microbiol **48:** 1253–1265

Chateigner-Boutin AL, Ramos-Vega M, Guevara-García A, Andrés C, de la Luz Gutiérrez-Nava M, Cantero A, Delannoy E, Jiménez LF, Lurin C, Small I, et al (2008) CLB19, a pentatricopeptide repeat protein required for editing of *rpoA* and *clpP* chloroplast transcripts. Plant J **56:** 590–602

Cheng ZF, Deutscher MP (2003) Quality control of ribosomal RNA mediated by polynucleotide phosphorylase and RNase R. Proc Natl Acad Sci USA **100:** 6388–6393

Chi W, Ma JF, Zhang DY, Guo JK, Chen F, Lu CM, Zhang LX (2008) The pentatricopeptide repeat protein DELAYED GREENING1 is involved in the regulation of early chloroplast development and chloroplast gene expression in Arabidopsis. Plant Physiol **147:** 573–584

Chi W, Mao J, Li QN, Ji DL, Zou MJ, Lu CM, Zhang LX (2010) Interaction of the pentatricopeptide-repeat protein DELAYED GREENING 1 with sigma factor SIG6 in the regulation of chloroplast gene expression in *Arabidopsis* cotyledons. Plant J **64:** 14–25

Coburn GA, Miao X, Briant DJ, Mackie GA (1999) Reconstitution of a minimal RNA degradosome demonstrates functional coordination between a 3′ exonuclease and a DEAD-box RNA helicase. Genes Dev **13:** 2594–2603

Cordin O, Banroques J, Tanner NK, Linder P (2006) The DEAD-box protein family of RNA helicases. Gene **367:** 17–37

de la Cruz J, Kressler D, Linder P (1999) Unwinding RNA in *Saccharomyces cerevisiae*: DEAD-box proteins and related families. Trends Biochem Sci **24:** 192–198

Dorne AM, Lescure AM, Mache R (1984) Site of synthesis of spinach chloroplast ribosomal proteins and formation of incomplete ribosomal particles in isolated chloroplasts. Plant Mol Biol **3:** 83–90

Edwards K, Kössel H (1981) The rRNA operon from *Zea mays* chloroplasts: nucleotide sequence of 23S rDNA and its homology with *E. coli* 23S rDNA. Nucleic Acids Res **9:** 2853–2869

Egebjerg J, Leffers H, Christensen A, Andersen H, Garrett RA (1987) Structure and accessibility of domain I of *Escherichia coli* 23 S RNA in free RNA, in the L24-RNA complex and in 50 S subunits: implications for ribosomal assembly. J Mol Biol **196:** 125–136

Fleischmann TT, Scharff LB, Alkatib S, Hasdorf S, Schöttler MA, Bock R (2011) Nonessential plastid-encoded ribosomal proteins in tobacco: a developmental role for plastid translation and implications for reductive genome evolution. Plant Cell **23:** 3137–3155

Fromont-Racine M, Senger B, Saveanu C, Fasiolo F (2003) Ribosome assembly in eukaryotes. Gene **313:** 17–42

Germain A, Herlich S, Larom S, Kim SH, Schuster G, Stern DB (2011) Mutational analysis of *Arabidopsis* chloroplast polynucleotide phosphorylase reveals roles for both RNase PH core domains in polyadenylation, RNA 3′-end maturation and intron degradation. Plant J **67:** 381–394

Gourse RL, Gaal T, Bartlett MS, Appleman JA, Ross W (1996) rRNA transcription and growth rate-dependent regulation of ribosome synthesis in *Escherichia coli*. Annu Rev Microbiol **50:** 645–677

Granneman S, Baserga SJ (2005) Crosstalk in gene expression: coupling and co-regulation of rDNA transcription, pre-ribosome assembly and pre-rRNA processing. Curr Opin Cell Biol **17:** 281–286

Harris EH, Boynton JE, Gillham NW (1994) Chloroplast ribosomes and protein synthesis. Microbiol Rev **58:** 700–754

Henras AK, Soudet J, Gérus M, Lebaron S, Caizergues-Ferrer M, Mougin A, Henry Y (2008) The post-transcriptional steps of eukaryotic ribosome biogenesis. Cell Mol Life Sci **65:** 2334–2359

Holmes KL, Culver GM (2005) Analysis of conformational changes in 16 S rRNA during the course of 30 S subunit assembly. J Mol Biol **354:** 340–357

Iost I, Dreyfus M (2006) DEAD-box RNA helicases in *Escherichia coli*. Nucleic Acids Res **34:** 4189–4197

Jankowsky E, Fairman ME (2007) RNA helicases: one fold for many functions. Curr Opin Struct Biol **17:** 316–324

Jenkins BD, Barkan A (2001) Recruitment of a peptidyl-tRNA hydrolase as a facilitator of group II intron splicing in chloroplasts. EMBO J **20:** 872–879

Kaczanowska M, Rydén-Aulin M (2007) Ribosome biogenesis and the translation process in *Escherichia coli*. Microbiol Mol Biol Rev **71:** 477–494

Keus RJA, Dekker AF, Kreuk KCJ, Groot GSP (1984) Transcription of ribosomal DNA in chloroplasts of *Spirodela oligorhiza*. Curr Genet **9:** 91–98

Kishine M, Takabayashi A, Munekage Y, Shikanai T, Endo T, Sato F (2004) Ribosomal RNA processing and an RNase R family member in chloroplasts of *Arabidopsis*. Plant Mol Biol **55:** 595–606

Kossen K, Uhlenbeck OC (1999) Cloning and biochemical characterization of *Bacillus subtilis* YxiN, a DEAD protein specifically activated by 23S rRNA: delineation of a novel sub-family of bacterial DEAD proteins. Nucleic Acids Res **27:** 3811–3820

Koussevitzky S, Stanne TM, Peto CA, Giap T, Sjögren LL, Zhao Y, Clarke AK, Chory J (2007) An *Arabidopsis thaliana virescent* mutant reveals a role for ClpR1 in plastid development. Plant Mol Biol **63:** 85–96

Kovtun Y, Chiu WL, Tena G, Sheen J (2000) Functional analysis of oxidative stress-activated mitogen-activated protein kinase cascade in plants. Proc Natl Acad Sci USA **97:** 2940–2945

Kressler D, Linder P, de La Cruz J (1999) Protein trans-acting factors involved in ribosome biogenesis in *Saccharomyces cerevisiae*. Mol Cell Biol **19:** 7897–7912

Leal-Klevezas DS, Martinez-Soriano JP, Nazar RN (2000) Transcription and processing map of the 4.5S-5S rRNA intergenic region (ITS3) from rapeseed (*Brassica napus*) chloroplasts. Plant Cell Rep **19:** 667–673

Lindahl L (1975) Intermediates and time kinetics of the in vivo assembly of Escherichia coli ribosomes. J Mol Biol **92:** 15–37

Maki Y, Tanaka A, Wada A (2000) Stoichiometric analysis of barley plastid ribosomal proteins. Plant Cell Physiol **41:** 289–299

Marchive C, Yehudai-Resheff S, Germain A, Fei Z, Jiang X, Judkins J, Wu H, Fernie AR, Fait A, Stern DB (2009) Abnormal physiological and molecular mutant phenotypes link chloroplast polynucleotide phosphorylase to the phosphorus deprivation response in Arabidopsis. Plant Physiol **151:** 905–924

Nierhaus KH (1991) The assembly of prokaryotic ribosomes. Biochimie **73:** 739–755

Nishimura K, Ashida H, Ogawa T, Yokota A (2010) A DEAD box protein is required for formation of a hidden break in Arabidopsis chloroplast 23S rRNA. Plant J **63:** 766–777

Rogalski M, Karcher D, Bock R (2008) Superwobbling facilitates translation with reduced tRNA sets. Nat Struct Mol Biol **15:** 192–198

Schluenzen F, Tocilj A, Zarivach R, Harms J, Gluehmann M, Janell D, Bashan A, Bartels H, Agmon I, Franceschi F, et al (2000) Structure of functionally activated small ribosomal subunit at 3.3 angstroms resolution. Cell **102:** 615–623

Schmitz-Linneweber C, Williams-Carrier RE, Williams-Voelker PM, Kroeger TS, Vichas A, Barkan A (2006) A pentatricopeptide repeat protein facilitates the trans-splicing of the maize chloroplast *rps12* pre-mRNA. Plant Cell **18:** 2650–2663

Shajani Z, Sykes MT, Williamson JR (2011) Assembly of bacterial ribosomes. Annu Rev Biochem **80:** 501–526

Sharpe Elles LM, Sykes MT, Williamson JR, Uhlenbeck OC (2009) A dominant negative mutant of the *E. coli* RNA helicase DbpA blocks assembly of the 50S ribosomal subunit. Nucleic Acids Res **37:** 6503–6514

Silverman E, Edwalds-Gilbert G, Lin RJ (2003) DExD/H-box proteins and their partners: helping RNA helicases unwind. Gene **312:** 1–16

Srivastava AK, Schlessinger D (1988) Coregulation of processing and translation: mature 5′ termini of *Escherichia coli* 23S ribosomal RNA form in polysomes. Proc Natl Acad Sci USA **85:** 7144–7148

Stelzl U, Nierhaus KH (2001) A short fragment of 23S rRNA containing the binding sites for two ribosomal proteins, L24 and L4, is a key element for rRNA folding during early assembly. RNA **7:** 598–609

Strittmatter G, Kössel H (1984) Cotranscription and processing of 23S, 4.5S

and 5S rRNA in chloroplasts from *Zea mays*. Nucleic Acids Res **12:** 7633–7647

Sun Q, Zybailov B, Majeran W, Friso G, Olinares PD, van Wijk KJ (2009) PPDB, the plant proteomics database at Cornell. Nucleic Acids Res **37:** D969–D974

Tiller N, Weingartner M, Thiele W, Maximova E, Schöttler MA, Bock R (2011) The plastid-specific ribosomal proteins of *Arabidopsis thaliana* can be divided into non-essential proteins and genuine ribosomal proteins. Plant J **69:** 302–316

Trubetskoy D, Proux F, Allemand F, Dreyfus M, Iost I (2009) SrmB, a DEAD-box helicase involved in *Escherichia coli* ribosome assembly, is specifically targeted to 23S rRNA in *vivo*. Nucleic Acids Res **37:** 6540–6549

Tumminia SJ, Hellmann W, Wall JS, Boublik M (1994) Visualization of protein-nucleic acid interactions involved in the in *vitro* assembly of the *Escherichia coli* 50 S ribosomal subunit. J Mol Biol **235:** 1239–1250

Walter M, Kilian J, Kudla J (2002) PNPase activity determines the efficiency of mRNA 3′-end processing, the degradation of tRNA and the extent of polyadenylation in chloroplasts. EMBO J **21:** 6905–6914

Wang Y, Duby G, Purnelle B, Boutry M (2000) Tobacco *VDL* gene encodes a plastid DEAD box RNA helicase and is involved in chloroplast differentiation and plant morphogenesis. Plant Cell **12:** 2129–2142

Watkins KP, Kroeger TS, Cooke AM, Williams-Carrier RE, Friso G, Belcher SE, van Wijk KJ, Barkan A (2007) A ribonuclease III domain protein functions in group II intron splicing in maize chloroplasts. Plant Cell **19:** 2606–2623

Williamson JR (2003) After the ribosome structures: how are the subunits assembled? RNA **9:** 165–167

Woody ST, Austin-Phillips S, Amasino RM, Krysan PJ (2007) The WiscDsLox T-DNA collection: an *Arabidopsis* community resource generated by using an improved high-throughput T-DNA sequencing pipeline. J Plant Res **120:** 157–165

Yamaguchi K, Beligni MV, Prieto S, Haynes PA, McDonald WH, Yates JR III, Mayfield SP (2003) Proteomic characterization of the *Chlamydomonas reinhardtii* chloroplast ribosome: identification of proteins unique to the 70 S ribosome. J Biol Chem **278:** 33774–33785

Yamaguchi K, Subramanian AR (2000) The plastid ribosomal proteins: identification of all the proteins in the 50 S subunit of an organelle ribosome (chloroplast). J Biol Chem **275:** 28466–28482

Yamaguchi K, Subramanian AR (2003) Proteomic identification of all plastid-specific ribosomal proteins in higher plant chloroplast 30S ribosomal subunit. Eur J Biochem **270:** 190–205

Yamaguchi K, von Knoblauch K, Subramanian AR (2000) The plastid ribosomal proteins: identification of all the proteins in the 30 S subunit of an organelle ribosome (chloroplast). J Biol Chem **275:** 28455–28465

Yu F, Liu X, Alsheikh M, Park S, Rodermel S (2008) Mutations in *SUPPRESSOR OF VARIEGATION1*, a factor required for normal chloroplast translation, suppress *var2*-mediated leaf variegation in *Arabidopsis*. Plant Cell **20:** 1786–1804

Yusupov MM, Yusupova GZ, Baucom A, Lieberman K, Earnest TN, Cate JHD, Noller HF (2001) Crystal structure of the ribosome at 5.5 A resolution. Science **292:** 883–896

Zhang LX, Paakkarinen V, van Wijk KJ, Aro EM (1999) Co-translational assembly of the D1 protein into photosystem II. J Biol Chem **274:** 16062–16067

Zybailov B, Friso G, Kim J, Rudella A, Rodríguez VR, Asakura Y, Sun Q, van Wijk KJ (2009) Large scale comparative proteomics of a chloroplast Clp protease mutant reveals folding stress, altered protein homeostasis, and feedback regulation of metabolism. Mol Cell Proteomics **8:** 1789–1810

Zybailov B, Rutschow H, Friso G, Rudella A, Emanuelsson O, Sun Q, van Wijk, KJ (2008) Sorting signals, N-terminal modifications and abundance of the chloroplast proteome. PLoS ONE **3:** e1994